

Aharonov-Bohm effect in the magnetoresistance of a multiwalled carbon nanotube with tunneling contacts

M.-G. Kang,¹ T. Morimoto,² N. Aoki,^{2,3} J.-U. Bae,¹ Y. Ochiai,^{2,3} and J. P. Bird¹

¹Department of Electrical Engineering, University at Buffalo, The State University of New York, Buffalo, New York 14260-1920, USA

²Graduate School of Science and Technology, Chiba University, 1-33 Yayoi-cho, Inage-ku, Chiba 263-8522, Japan

³Department of Electronics and Mechanical Engineering, Chiba University, 1-33 Yayoi-cho, Inage-ku, Chiba 263-8522, Japan

(Received 22 August 2007; revised manuscript received 20 December 2007; published 24 March 2008)

We study the magnetoresistance (MR) of a multiwalled carbon nanotube (MWNT) as a function of the angle (θ_{tilt}) between the external field (B_{ext}) and the MWNT axis. With B_{ext} oriented along the nanotube axis, its MR exhibits two symmetric (with respect to zero field) sharp minima that shift to higher B_{ext} as this field is rotated away from the axis. We suggest that these minima are associated with a cancellation of the nanotube effective flux as predicted by Nakanishi and Ando [J. Phys. Soc. Jpn. **74**, 3027 (2005)].

DOI: [10.1103/PhysRevB.77.113408](https://doi.org/10.1103/PhysRevB.77.113408)

PACS number(s): 73.63.Fg, 78.66.Tr, 75.47.-m, 73.22.-f

Carbon nanotubes (CNTs) have attracted interest as unique one-dimensional conductors with outstanding electrical properties.^{1,2} In this Brief Report, we focus on some of the effects that can arise in their conductivity, when a magnetic field induces an enclosed Aharonov-Bohm (AB) flux. The response to such a flux has been studied in many experiments,³⁻¹³ which have established its ability to coherently modulate the wave function and to thereby change the electrical and/or optical response of the CNT. In theoretical work, Ando and co-workers have emphasized the modifications to the band structure that such a flux may cause.^{2,14-18} They have shown that, when rolling graphene to form a CNT, one induces a nonzero *effective flux* (φ_e , in units of the flux quantum h/e) that opens a gap (proportional to φ_e) in the graphene spectrum.¹⁸ A magnetic field should cause this gap to vanish, however, if the external flux (φ_{ext}) becomes equal to $\pm\varphi_e$. At this condition, backscattering is suppressed and one therefore expects to observe a peak in the CNT magnetoconductance, which should rise to infinity in the absence of scattering.¹⁸

In this Brief Report, we present a magnetoresistance (MR) study of a multiwalled CNT (MWNT) with tunneling contacts, which may show evidence for the AB effect predicted in Ref. 18. The use of tunneling contacts in this work is motivated by the idea of performing a spectroscopy of the CNT density of states.¹⁹ Our experiment reveals two main MR features, which evolve differently as the angle (θ_{tilt}) between the external field (B_{ext}) and the CNT axis is varied. The first is a pair of sharply pronounced dips, which occur at $\sim\pm 3$ T for $\theta_{\text{tilt}}=0^\circ$ but which shift to higher B_{ext} as θ_{tilt} is increased. This evolution follows a $\sim 1/\cos\theta_{\text{tilt}}$ behavior, indicating that it is likely associated with the AB flux threading the CNT cross section. The second feature is a negative-MR peak at $B_{\text{ext}}=0$ T that is found to be *independent* of θ_{tilt} . We discuss these two features in terms of separate phenomena of band modulation and weak localization, which could exhibit very different geometric dependences on the external magnetic field.

Atomic-force microscope (AFM) images of our device are shown in the insets of Figs. 1(a) and 1(b). The device was fabricated by dispersing a dichloroethane solution containing MWNTs (Vacuum Metallurgical Co., Ltd.) onto a conducting

p-type Si substrate with a 600 nm SiO₂ cap layer. Electron-beam lithography (EBL) was then used to form metallic (Ti/Au: 15/35 nm thick) contacts, with a separation of 2.3 μm . AFM measurements indicate a CNT diameter of 15 ± 1 nm, so that an external field of ~ 23 T should be needed to induce an AB flux of one quantum. For metallic nanotubes, however, the effective flux should be very small ($|\varphi_e| < 1$),^{15,16} allowing one to easily achieve the condition $\varphi_{\text{ext}} = \pm\varphi_e$. The distinction between these two field scales will be important below when we discuss our experimental results. As can also be seen in the inset of Fig. 1(b), a second EBL step was used to pattern six nanomagnets (Ni/Au: 45/5 nm thick) on top of the MWNT. The purpose of this array was to explore a proposal for hysteretic memory in nanowires, using the fringing fields from such nanomagnets.²⁰ No hysteresis was observed in our experiments, however, and we return to comment on this further below.

Our CNT device was mounted in the rotating holder of a variable-temperature (4.2–100 K) cryostat, and its MR was measured by low-frequency (~ 11 Hz) lock-in detection. In Fig. 1(a), we show the temperature-dependent variation of the CNT resistance (R_{2T}) measured with a constant drive current of 3.3 nA. R_{2T} increases from ~ 50 K Ω at 300 K and saturates at ~ 17 M Ω below 40 K, due to the limited input impedance of the lock-in amplifier. Indeed, Fig. 1(b) plots the dc current-voltage characteristic of the CNT at 4.2 K and shows the nonlinear behavior typical of back-to-back Schottky junctions formed by insulating contacts. These data also indicate that the conductance can be significantly increased by applying a nonlinear source bias, and in our experiment we therefore study the MR with a fixed ac drive voltage of 500 mV rms. In Fig. 1(a), we also plot the temperature dependence of R_{2T} for this excitation and see that R_{2T} now saturates at ~ 1 M Ω (*not* an instrument-related effect). In Fig. 1(c), we show the MR measured at 4.2 K with B_{ext} applied along the CNT ($\theta_{\text{tilt}}=0^\circ$). Different data points correspond to sweeping B_{ext} in opposite directions and the data are highly reproducible with no hysteresis. Increasing $|B_{\text{ext}}|$ from zero, negative MR is first observed up to $B_{\text{ext}} = \pm 3$ T, at which point, however, an *extremely sudden* reversal occurs and a positive MR is then observed all the way to

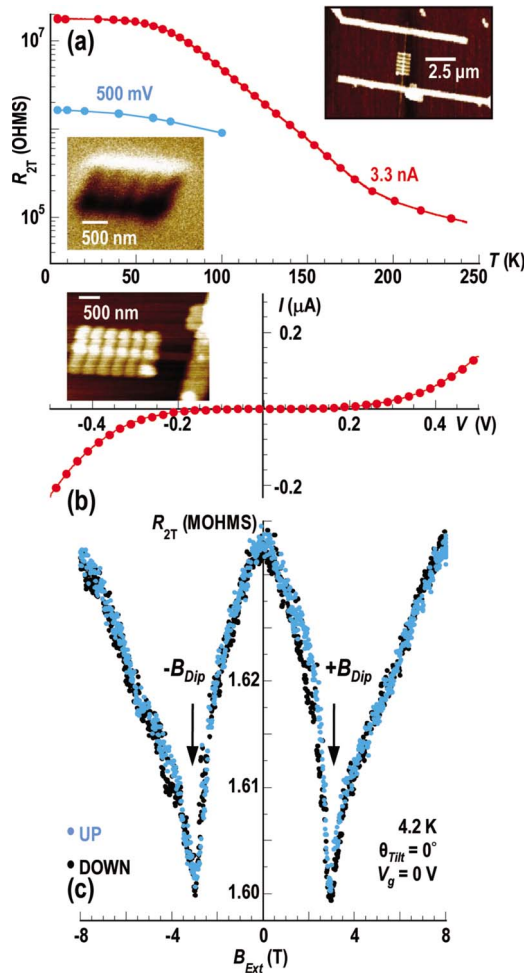


FIG. 1. (Color online) (a) $R_{2T}(T)$ for the CNT device. Red circles (gray), measured with constant drive current of 3.3 nA. Blue circles (dark gray), measured with a constant voltage of 500 mV. These data were extracted from our T -dependent MR measurements. Upper inset: AFM image of the CNT device showing its contacts and the periodic gate array. Lower inset: Magnetic-force microscopy image of a test pattern of an array of five nanomagnets. Bright and dark regions show magnetic poles and the single-domain nature of the nanomagnets. (b) Source-drain current-voltage characteristic of the CNT device at 4.2 K. Inset: AFM image of the CNT device in close-up. (c) MR measurement of the CNT device at 4.2 K. Results for sweeps in opposite directions are indicated.

± 8 T [we define the values of B_{ext} at which the MR minima occur as $\pm B_{dip}$, as indicated in Fig. 1(c)]. In measurements where we varied the excitation voltage between 0.1 and 1 V rms (not shown), we found in all cases a similar MR structure, with deep minima occurring at the same values of B_{dip} .

Figure 2(a) shows the evolution of the MR as θ_{tilt} is varied from 0° to 40° . As B_{ext} is rotated away from the CNT axis, the MR dips shift to higher B_{ext} . At the same time, however, the zero-field peak seen for $-2 < B_{ext} < +2$ T remains independent of θ_{tilt} . In Fig. 2(b), we plot the variation of (the field-polarity averaged value of) B_{dip} as a function of θ_{tilt} . Red data plot the value of $|B_{ext}|$ for which the minima are seen, while the blue data were obtained by multiplying these values by $\cos \theta_{tilt}$. The blue data therefore represent the value

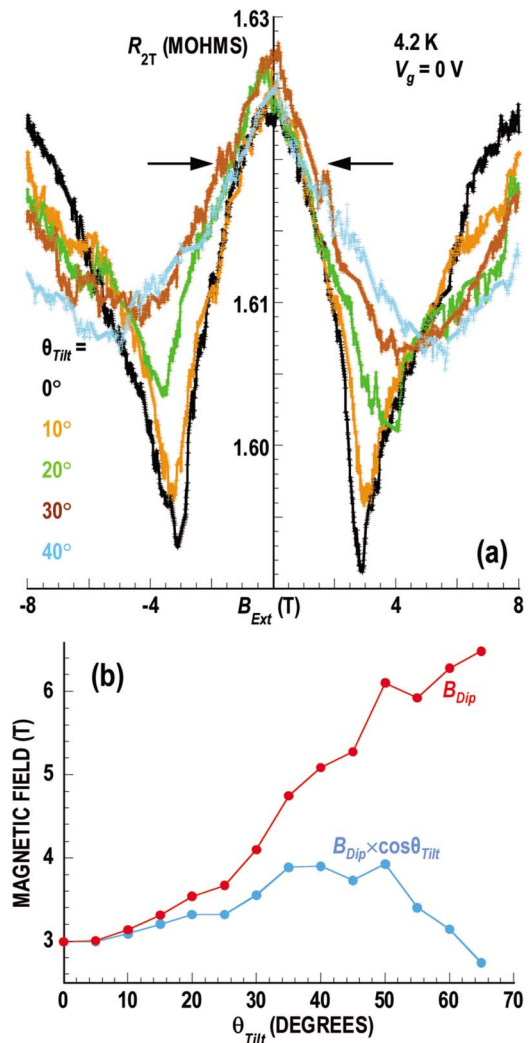


FIG. 2. (Color online) (a) Evolution of the MR as a function of θ_{tilt} . Arrows denote a central peak that is invariant to the change of θ_{tilt} . (b) Red (gray) data indicate the value of the external magnetic field at which the symmetric MR dips are observed, while blue (dark gray) data indicate the corresponding value of the field component along the nanotube length ($B_{ext} \cos \theta_{tilt}$).

of the external-field component along the CNT axis, when the MR dips occur. These data indicate that the field position of the dips scales fairly well as $1/\cos \theta_{tilt}$, although there is also a systematic deviation from this dependence. A similar deviation was noted in a previous study³ and was suggested to be due to a possible misalignment of the CNT and field axes for $\theta_{tilt}=0^\circ$. Actually, in our device, there is a $\sim 6^\circ$ misalignment of the CNT axis relative to the alignment marks on the wafer. In spite of these issues, however, we believe that the behavior of Fig. 2(b) indicates that the MR dips are associated with the AB flux (φ_{ext}) threading the CNT cross section.

For our CNT device, the field required to add one flux quantum to its cross section is ~ 23 T. The MR dips we observe, however, involve a normal field of ~ 3 T, corresponding to a flux of just $\sim 0.13(h/e)$. This suggests that the origin of these dips may be the cancellation of φ_e by B_{ext} , as suggested by Ando and co-workers.^{2,14-18} For metallic nano-

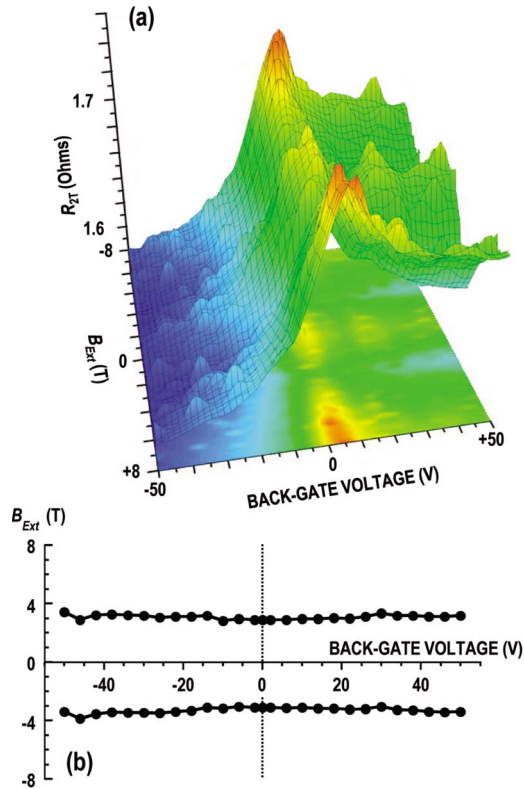


FIG. 3. (Color online) (a) Variation of R_{2T} as a function of magnetic field and back-gate voltage for $\theta_{\text{tilt}}=0^\circ$ at 4.2 K. (b) The variation of B_{dip} as function of back-gate voltage.

tubes, the value of φ_e should be much smaller than unity, consistent with our observation that the MR dips correspond to $\varphi_{\text{ext}} \sim 0.13$. When $\varphi_{\text{ext}} = \varphi_e$ is satisfied, the recovery of a linear dispersion is expected to lead to an increase of the conductance to infinity, at least in a perfect nanotube.¹⁸ By accounting for short-range scatterers, however, a MR similar to that which we observe was obtained (see, for example, Figs. 3 and 4 of Ref. 18, which plot the *magnetoconductance* for different electron densities and impurity-scattering strength).

Nakanishi and Ando¹⁸ have also calculated the dependence of the MR dip on electron density and have found that its amplitude is modulated while its field position is invariant. The latter observation reflects the structurally related origin of φ_e . In Fig. 3, we show the variation of the CNT MR as a function of the back-gate voltage (V_g) applied to its conducting Si substrate. It is clear from this figure that the MR dips persist over the entire range of V_g and that B_{dip} does not change significantly [Fig. 3(b)], consistent with the discussion above. Note also the weak effect of the gate voltage, which modulates R_{2T} by less than 10% for a total voltage swing of 100 V. This seems consistent with our idea that we indeed have a metallic CNT, which is contacted by high-resistance contacts.

Another feature of Fig. 2(a) is the zero-field MR peak, which is independent of θ_{tilt} for $|B_{\text{ext}}| < 2$ T. One idea is that this arises from weak localization (WL), due to trajectories enclosing fixed area that evolve with θ_{tilt} ,^{5,6} and is superimposed upon the larger resistance variation arising from the

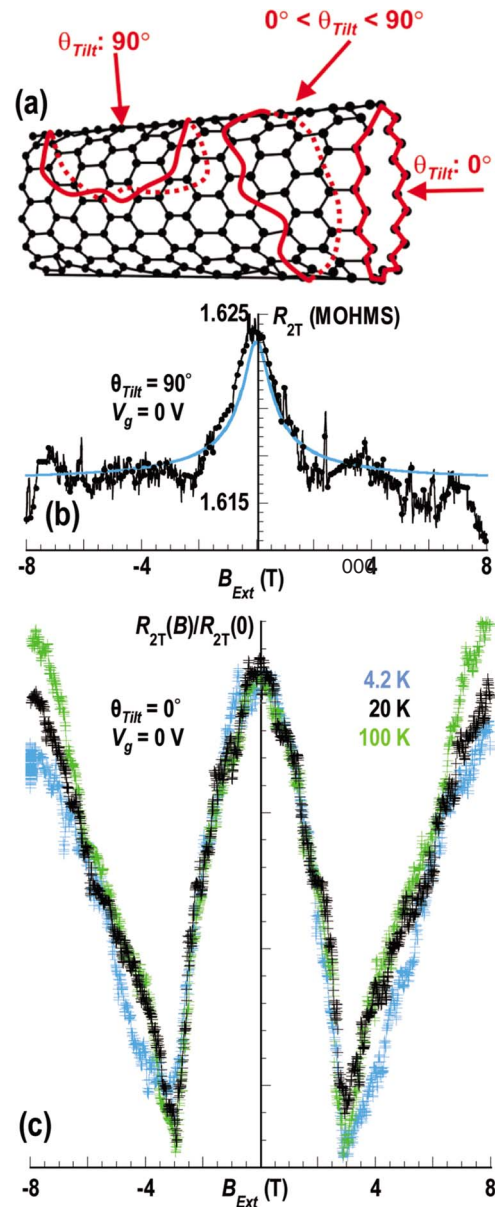


FIG. 4. (Color online) (a) Schematic illustration of different trajectories that could contribute to a weak-localization process as θ_{tilt} is varied. Arrows indicate the direction of B_{ext} . (b) The MR (circles) for $\theta_{\text{tilt}}=90^\circ$ at 4.2 K with a best fit to Eq. (1) (solid line). (c) Relative MR at three different temperatures. $R_{2T}(B=0)=1.64$, 1.61, and 0.90 M Ω at 4.2 (gray), 20 K (black), and 100 K (dark gray), respectively

AB effect. This idea is expressed in Fig. 4(a), which suggests possible trajectories involved in WL; as B_{ext} is rotated away from the CNT axis, one can always identify characteristic trajectories that are threaded by an AB flux. Such behavior might account for the angular invariance of the central peak. (Indeed, Ando and Nakanishi showed in Ref. 18 that the AB effect they discussed should survive for moderate impurity scattering, so that it is possible that this effect could coexist with WL.) To check this idea, in Fig. 4(b), we perform a two-parameter (W and l_φ) fit of the MR for $\theta_{\text{tilt}}=90^\circ$ (where there is no AB flux threading the tube) to the form for one-dimensional WL,^{21–23}

$$\Delta G_{WL} = -\frac{e^2}{\pi\hbar L} \left[l_\phi^{-2} + \frac{(WeB)^2}{3\hbar^2} \right]^{-0.5}, \quad (1)$$

where l_ϕ is the phase-breaking length and L is the contact spacing. In conventional WL theory, W is the width of the one-dimensional conductor, although, in applying this formula to CNT MR, it has been found necessary to treat it as a free parameter whose value can be smaller than the CNT diameter.²⁴ In Fig. 4(b), we show quite good agreement between the experimental MR for $\theta_{\text{tilt}}=90^\circ$ and a fit to Eq. (1) (with $W=2.4$ nm and $l_\phi=1050$ nm). The value for W is a factor of 6 smaller than the outer diameter of the nanotube and, although a reduced value for W was found in Ref. 24, the discrepancy with the nanotube size in that case was just a factor of ~ 2 . The value of l_ϕ that we infer is also significantly longer than that reported elsewhere.^{24,25} While the results thus far were obtained at 4.2 K, we have also measured the temperature dependence of the MR (for $\theta_{\text{tilt}}\sim 0^\circ$) up to 100 K [Fig. 4(c), the MR is normalized here in terms of its zero-field value] and find only a small reduction (by $\sim 10\%$) in the MR. If the data of Fig. 4(c) are interpreted in terms of WL, they would point to a temperature-independent l_ϕ to beyond 100 K, behavior very different to that reported previously.^{21,24} The low-field MR may therefore be due to some other effect than WL (the angular invariance of this MR could indicate a phenomenon unrelated to the orbital effect of the magnetic field, such as a lifting of Zeeman degeneracy). Further studies of this issue are required but are beyond the scope of this Brief Report.

While our device features a periodic array of nanomagnets, no MR hysteresis was found, even though magnetic-

force microscopy confirmed the single-domain nature of these nanomagnets [Fig. 1(a)]. One reason for this could be that the large B_{ext} we apply may effectively swamp the nanomagnet fringing fields. In recent measurements of GaAs wires bridged by nanomagnets, significant MR hysteresis was only observed when B_{ext} was applied in the plane of the wire, when the Lorentz force due to B_{ext} vanishes.²⁶ In the CNT device, however, it appears that there is no value of θ_{tilt} for which such a condition can be achieved, which may therefore obscure the fringing fields from the nanomagnets.

In conclusion, we have studied the MR of a MWNT while varying the angle between the external field and the nanotube axis. With this field oriented along the CNT axis, its MR was found to exhibit two sharp minima at $\sim \pm 3$ T, which shifted to increasing magnetic field as B_{ext} was rotated away from the CNT axis. We have suggested that these features are associated with the cancellation of the effective flux predicted by Ando and co-workers, in which case our results imply $\varphi_e \sim 0.13$ (in units of h/e), a reasonable result for a metallic nanotube. The second MR feature was found to be a zero-field peak that was insensitive to the variation of θ_{tilt} . We have suggested that this may arise from weak localization, due to trajectories that evolve as θ_{tilt} is varied.

Work at Buffalo was supported by the Department of Energy (DE-FG03-01ER45920) and the National Science Foundation (ECS-0224163) (M.G.K.). Work at Chiba University was supported by the Graduate School of Science and Technology, the Chiba University 21COE program ‘‘Frontiers of Super-Functionality Organic Devices,’’ and in part by a grant-in-aid from the Japan Society for Promotion of Science (Nos. 16306001 and 19204030).

¹ *Carbon Nanotubes: Synthesis, Structure, Properties, and Applications*, edited by M. S. Dresselhaus, G Dresselhaus, and Ph. Avouris, Springer Topics in Applied Physics Vol. 80 (Springer, Berlin, 2001).

² T. Ando, J. Phys. Soc. Jpn. **74**, 777 (2005).

³ A. Fujiwara *et al.*, Phys. Rev. B **60**, 13492 (1999).

⁴ A. Bachtold *et al.*, Nature (London) **397**, 673 (1999).

⁵ C. Schonenberger *et al.*, Appl. Phys. A: Mater. Sci. Process. **69**, 283 (1999).

⁶ H. R. Shea, R. Martel, and Ph. Avouris, Phys. Rev. Lett. **84**, 4441 (2000).

⁷ Jeong-O. Lee *et al.*, Phys. Rev. B **61**, R16362 (2000).

⁸ J. Cao, Q. Wang, M. Rolandi, and H. Dai, Phys. Rev. Lett. **93**, 216803 (2004).

⁹ S. Zaric Gordana *et al.*, Science **304**, 1129 (2004).

¹⁰ U. C. Coskun *et al.*, Science **304**, 1132 (2004).

¹¹ G. Fedorov *et al.*, Phys. Rev. Lett. **94**, 066801 (2005).

¹² H. T. Man and A. F. Morpurgo, Phys. Rev. Lett. **95**, 026801 (2005).

¹³ S. Zaric *et al.*, Phys. Rev. Lett. **96**, 016406 (2006).

¹⁴ H. Ajiki and T. Ando, J. Phys. Soc. Jpn. **62**, 2470 (1993).

¹⁵ H. Ajiki and T. Ando, Physica B **201**, 349 (1994).

¹⁶ T. Ando, Semicond. Sci. Technol. **15**, R13 (2000).

¹⁷ T. Ando, J. Phys. Soc. Jpn. **69**, 1757 (2000).

¹⁸ T. Nakanishi and T. Ando, J. Phys. Soc. Jpn. **74**, 3027 (2005).

¹⁹ W. Yi *et al.*, Phys. Rev. Lett. **91**, 076801 (2003).

²⁰ J.-F. Song, J. P. Bird, and Y. Ochiai, J. Phys.: Condens. Matter **17**, 5263 (2005).

²¹ C. Strunk, B. Stojetz, and S. Roche, Semicond. Sci. Technol. **21**, S38 (2006).

²² B. L. Altshuler, A. G. Aronov, and D. E. Khmel'nitsky, J. Phys. C **15**, 7367 (1982).

²³ J. J. Lin and J. P. Bird, J. Phys.: Condens. Matter **14**, R501 (2002).

²⁴ C. Schonenberger *et al.*, Appl. Phys. A: Mater. Sci. Process. **69**, 283 (1999).

²⁵ K. Liu, P. Avouris, R. Martel, and W. K. Hsu, Phys. Rev. B **63**, 161404(R) (2001).

²⁶ J.-U. Bae *et al.*, Appl. Phys. Lett. **91**, 022105 (2007).